Int. J. Heat Mass Transfer. Vol. 22, pp. 575–584
Pergamon Press Ltd. 1979. Printed in Great Britain

GENERALIZED CORRELATIONS OF CRITICAL HEAT FLUX FOR THE FORCED CONVECTION BOILING IN VERTICAL UNIFORMLY HEATED ANNULI

Y. KATTO
Department of Mechanical Engineering, University of Tokyo,
Hongo, Bunkyo-ku, Tokyo, Japan

(*Received* 15 *May* 1978)

Abstract—Following the analytical procedure of the same principle as that applied by the author to the analysis of critical heat flux (CHF) for round tubes, existing experimental data of CHF in annuli with inside heating are analyzed to yield a generalized correlation of CHF proper to this type of heating. As for annuli with outside heating, it is shown that CHF can be readily predicted by utilizing the author's generalized correlation of CHF for round tubes. The prediction of CHF in both cases mentioned above can be established by employing the heated equivalent diameter alone as the representative diameter of annuli. Finally, the case of bilaterally heated annuli is also discussed, and an approximate method for the prediction of CHF in L- and H-regime is presented, while it is suggested that the interference between two walls disappears for CHF in HP-regime.

NOMENCLATURE

- d, inner diameter of round tube [m];
- d_{he}, heated equivalent diameter [m];
- d_i, outer diameter of rod of annulus [m];
- d_0, inner diameter of shroud tube of annulus [m];
- G, mass velocity [kg/m^2 s];
- H_{fg}, latent heat of evaporation [J/kg];
- ΔH_i, enthalpy of inlet subcooling [J/kg];
- K, parameter for inlet subcooling effect, equation (14);
- l, length of heated rod or tube [m];
- p, absolute pressure [bar];
- q_c, critical heat flux [W/m^2];
- q_{c0}, q_c for $\Delta H_i = 0$ [W/m^2].

Greek symbols

- α, fraction of total power added to shroud tube;
- ρ_l, density of liquid [kg/m^3];
- ρ_v, density of vapor [kg/m^3];
- σ, surface tension [N/m];
- χ_{ex}, exit quality.

1. INTRODUCTION

THE PRESENT paper deals with the critical heat flux (CHF) for the forced convection boiling in annular channels in the conditions that the fluid fed to the channels is subcooled (inclusive of saturated liquid in the limit) and the flow is stable with no oscillations. For CHF of water in annuli with inside heating, where the inside rod is heated and the shroud tube unheated, Barnett [1] compiled 724 experimental data at the pressure of 69.0 bars from 8 sources, and later [2] compiled 106 new data at the same pressure from 3 sources. Janssen *et al.* [3] made experiments of water at 41.4–100.0 bars (among their data, those at 69.0 bars were compiled in [1]), while the study of Little [4] included experiments of water at 51.7–69.0 bars. As for pure fluids other than water, the study of Stevens *et al.* [5] included experiments of Freon-12 at 8.1–10.7 bars, while Ahmed *et al.* [6] presented 418 experimental data of Freon-12 at 10.7–16.4 bars. On the other hand, under conditions comprising inside heating (where the rod is heated and the shroud unheated), outside heating (where the rod is unheated and the shroud heated), and bilateral heating (where the rod and shroud are heated), experiments of annuli were made for water, in which Becker *et al.* [7] (p = 8.3–36.8 bars) and Jensen *et al.* [8] (p = 69.0 bars) showed that CHF on one side wall was affected by the heating of the other side wall, whereas Ornatskiy *et al.* [9] (p = 172–216 bars) and Tolubinskiy *et al.* [10] (p = 150–200 bars) found no effects of the other side wall heating on CHF. In another study of Ornatskiy *et al.* [11] were also included experiments of water at 98.1–186.5 bars for outside heating.

As for the correlation of experimental data, Barnett [1], Janssen *et al.* [3], Tong *et al.* [12], Bertolletti *et al.* [13], Becker [14] and Hewitt [15] developed empirical correlations of CHF for water flowing in annuli with inside heating, while Ahmad *et al.* [6, 16] presented a kind of generalized correlation of CHF for inside heating in relation to their study of CHF modeling. In addition, for common use without discrimination between the inside and the outside heating, Tolubinskiy *et al.* [17] presented an empirical correlation of CHF for water, and Ornatskiy [18] a kind of generalized

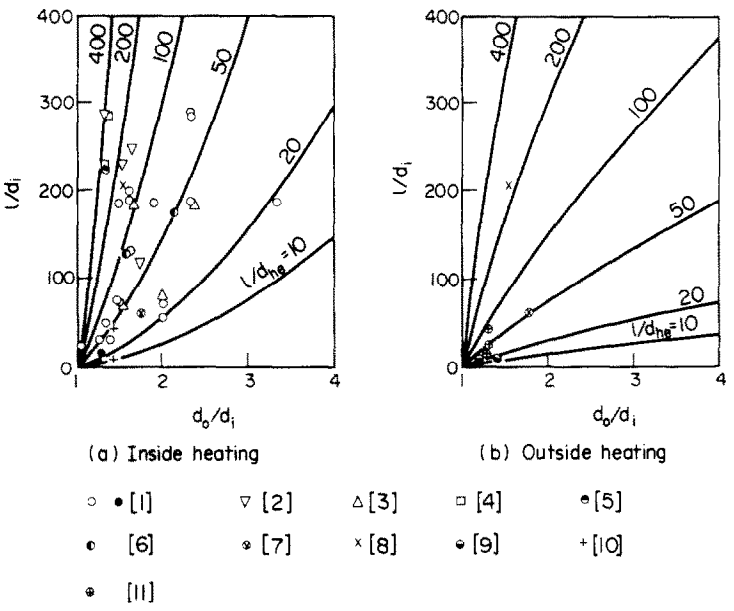

FIG. 1. Geometrical conditions and heated equivalent diameter for annuli.

correlation of CHF, but it must be noted that the former correlation implies CHF of natural convection boiling as a base and the latter correlation of CHF is composed including the gravitational acceleration g to make a dimensionless group.

Recently, the author developed a generalized correlation of CHF for round tubes [19] and showed its wide applicability [20]. The present paper reports the results obtained when the analytical procedure of the same principle is extended to annuli, which have two diameters as against one diameter in round tubes.

2. HEATED EQUIVALENT DIAMETER

Heated equivalent diameter d_{he} plays a dominant role in correlating CHF of annuli as it will be seen later, and a brief description of d_{he} is given here for convenience. Generally, heated equivalent diameter d_{he} is defined for the cross-section of any one-dimensional channel as:

$$d_{he} = (4 \times \text{flow area})/(\text{heated perimeter}), \quad (1)$$

and in case of uniform heat flux, the following heat balance relation holds for channels of length l:

$$\frac{q_c}{GH_{fg}} \cdot \frac{4l}{d_{he}} = \frac{\Delta H_i}{H_{fg}} = \chi_{ex}. \quad (2)$$

On the other hand, from the definition of equation (1), heated equivalent diameter d_{he} for annuli having the rod of diameter d_i and the shroud tube of diameter d_0 is determined as follows:

for inside heating:

$$\frac{l}{d_{he}} = \frac{l}{d_i} \cdot \frac{1}{(d_0/d_i)^2 - 1}; \quad (3)$$

for outside heating:

$$\frac{l}{d_{he}} = \frac{l}{d_i} \cdot \frac{d_0/d_i}{(d_0/d_i)^2 - 1}. \quad (4)$$

Equations (3) and (4) are illustrated in Fig. 1(a) and (b) respectively, and geometrical conditions of annuli employed in the experiments of [1–11] are also shown in Fig. 1. It should be noticed in Fig. 1 that when d_0/d_i is near unity, even a slight change of d_0/d_i causes a great change of l/d_{he}, and besides, that the origin of Fig. 1(a) and (b) ($l/d_i = 0$, $d_0/d_i = 1$) is a singular point corresponding to rectangular channels, where l/d_{he} becomes indefinite in equations (3) and (4) unless the annular width $(d_0 - d_i)/2$ is kept constant.

3. CHF FOR INSIDE HEATING

This chapter deals with CHF in case of annuli with inside heating, where the inside rod is heated and the shroud unheated.

3.1. *Relationship between* q_c *and* ΔH_i

When the relationship between q_c and ΔH_i is surveyed on the experimental data of [1–6], it is found that when the mass velocity G is low, the linear relationship (type A in Fig. 2) is observed, whereas when G is sufficiently high, the non-linear relationship (type B generally, and also type b occasionally in Fig. 2) appears. This phenomenological nature of CHF in annuli with inside heating is the same as that observed in round tubes [19], with the exception of occasional appearance of $q_c - \Delta H_i$ relationship of type b in Fig. 2.

3.2. *The clue for analyzing* q_{c0} *data*

Experiments represented by two black circular symbols near the origin of Fig. 1(a) give rather abnormal data compared with the other experiments, so that only these data are excluded from the analysis in the present paper. The analytical procedure employed in the study of round tubes [19] for correlating q_{c0}, which is obtained by extrapolating q_c

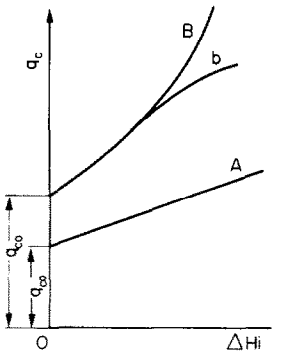

FIG. 2. Relationship between q_c and ΔH_i.

as $\Delta H_i \to 0$, is extended to the case of annuli as follows. Namely, keeping d_i constant in annuli, the limit as $d_0 \to \infty$ is assumed, when there is a possibility of obtaining a correlation of the following form:

$$\frac{q_{c0}}{GH_{fg}} = \text{const.}\left(\frac{\rho_v}{\rho_l}\right)^{0.133}\left(\frac{\sigma\rho_l}{G^2 l}\right)^{1/3}. \quad (5)$$

On the other hand, keeping d_i constant, the limit as $d_0 \to d_i$ is assumed, when the correlation equation should take the following form:

$$\frac{q_{c0}}{GH_{fg}} \cdot \frac{l}{d^*} = \text{const.}\left(\frac{\rho_l}{\rho_v}\right)^{a}\left(\frac{\sigma\rho_l}{G^2 l}\right)^{b}, \quad (6)$$

where d^* is a quantity having dimension of diameter.

In many of the existing correlation equations for CHF in annuli, hydraulic equivalent diameter is used either independently or jointly with heated equivalent diameter. However, the hydraulic diameter is primarily a quantity closely related to the friction of viscous flow in channels, so that if CHF is a phenomenon on which the viscosity has only the secondary effect (as assumed in [19] and [20]), the hydraulic diameter cannot be one of the important factors for CHF. On the contrary, the heated equivalent diameter is an indispensable quantity relating to the heat balance of uniformly heated channels [see equation (2)]. Therefore, it may be worthwhile to substitute l/d_{he} in equation (3) for l/d^* in equation (6), and in this case, one can have the following equation which approaches equations (5) and (6) respectively as $d_0 \to \infty$ and $d_0 \to d_i$.

$$\frac{q_{c0}}{GH_{fg}} = \text{const.}\left(\frac{\rho_v}{\rho_l}\right)^{0.133}\left(\frac{\sigma\rho_l}{G^2 l}\right)^{1/3} \times \frac{1}{1+\text{const.}\left(\frac{\rho_l}{\rho_v}\right)^{m}\left(\frac{\sigma\rho_l}{G^2 l}\right)^{n}\frac{l}{d_{he}}}. \quad (7)$$

As regards equation (7), it should be noted that when d_i is kept constant in equation (3), l/d_{he} tends to zero in the limit as $d_0 \to \infty$, and l/d_{he} tends to infinity in the limit as $d_0 \to d_i$.

Then, typical examples for the empirical relation between $(\sigma\rho_l/G^2 l)^{1/3}/(q_{c0}/GH_{fg})$ and $\sigma\rho_l/G^2 l$ which is found from the data of q_{c0} for constant ρ_v/ρ_l and l/d_{he} are shown in Fig. 3. It is noticed in Fig. 3 that similarly as in case of round tubes, characteristic regimes can be classified as follows: H-regime where the ordinate value is kept constant, L-regime where the ordinate value increases with $\sigma\rho_l/G^2 l$, and N-regime where the ordinate value decreases with $\sigma\rho_l/G^2 l$, and at the same time, the non-linear $q_c - \Delta H_i$ relationship (a black triangular symbol in Fig. 3 shows the corresponding datum) appears.

3.3. *Analysis of* q_{c0} *data in H-regime*

Consulting equation (7), all the data of q_{c0} in H-regime obtained from [1–6] are correlated as in Fig. 4. The data show scattering somewhat, but almost all the data can be correlated within errors less than $\pm 10\%$ by

$$\frac{q_{c0}}{GH_{fg}} = 0.12\left(\frac{\rho_v}{\rho_l}\right)^{0.133}\left(\frac{\sigma\rho_l}{G^2 l}\right)^{1/3} \times \frac{1}{1+0.0081 l/d_{he}}. \quad (8)$$

It is noted that a constant relating to l/d_{he} on the RHS of equation (8) is larger by as much as 2.6 times than that in the H-regime correlation equation for round tubes [equation (A.2) in Appendix].

3.4. *Analysis of* q_{c0} *data in L-regime*

Few data in L-regime can be found in [1–6].

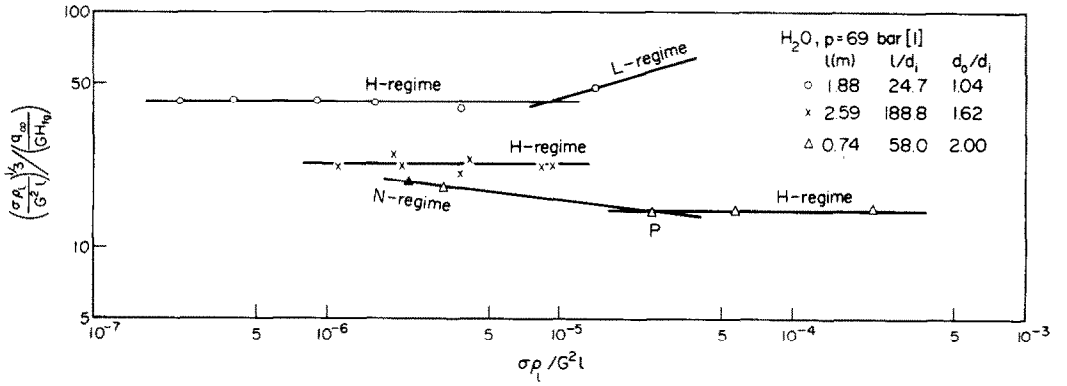

FIG. 3. Characteristics of q_{c0} under the conditions of constant ρ_v/ρ_l and l/d_{he}.

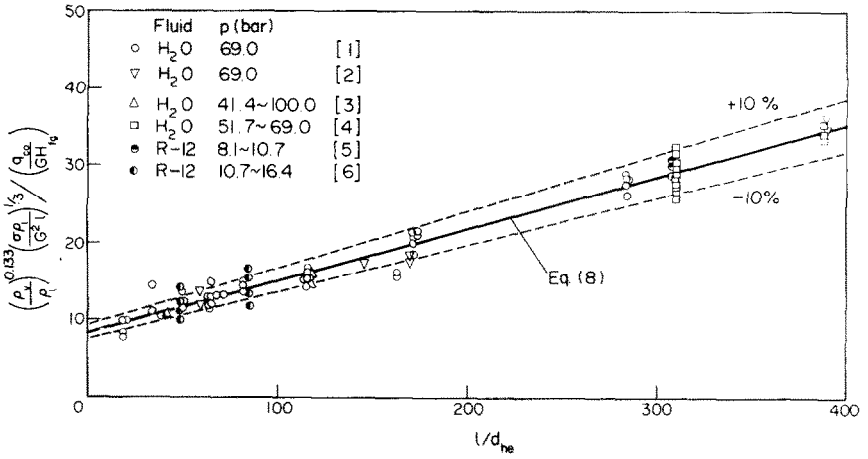

FIG. 4. Nondimensional correlation of q_{c0} in H-regime.

However, consulting the L-regime correlation equation for round tubes [that is, equation (A.1) in Appendix], and employing l/d_{he} of equation (3) instead of l/d, the data are correlated as in Fig. 5, to give the correlation equation:

$$\frac{q_{c0}}{GH_{fg}} = 0.25\left(\frac{\sigma\rho_l}{G^2 l}\right)^{0.043}\frac{1}{l/d_{he}}. \tag{9}$$

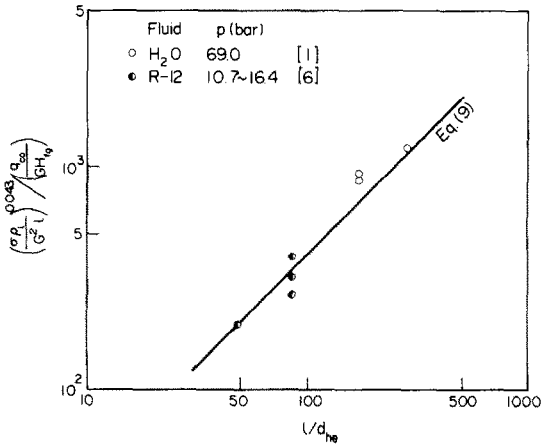

FIG. 5. Nondimensional correlation of q_{c0} in L-regime.

Equation (9) is regarded as a tentative equation due to insufficiency of available data, but having the same form as that of equation (A.1), it may suggest that the deficiency of liquid on the heated surface is responsible for CHF in L-regime similarly as in case of round tubes [20].

3.5. *Analysis of* q_{c0} *data in N-regime*

Strictly speaking, N-regime is the region where the non-linear $q_c - \Delta H_i$ relationship takes place, but as shown by the slant line on the LHS of the point P in Fig. 3, a part of H-regime (that may be called quasi N-regime) shows the same characteristics as those of N-regime for the variation of q_{c0}, so that q_{c0} data in both N-regime and quasi N-regime will be dealt with together. One cannot find sufficiently many data for these regimes in [1–6], but consulting equations (A.2) and (A.3) in Appendix and equation (8), the data are correlated in Fig. 6, to give the correlation equation:

$$\frac{q_{c0}}{GH_{fg}} = 0.22\left(\frac{\rho_v}{\rho_l}\right)^{0.133}\left(\frac{\sigma\rho_l}{G^2 l}\right)^{0.433} \times \frac{(l/d_{he})^{0.171}}{1+0.0081 l/d_{he}}. \tag{10}$$

It is particularly noticeable that the exponent of l/d_{he} on the RHS of equation (10) is smaller as much as 0.63 times than that in equation (A.3) in Appendix. The data in N-regime show considerable scattering in Fig. 6, but it may be of use to note that similar scattering of data is also observed in N-regime of round tubes (cf. [19]).

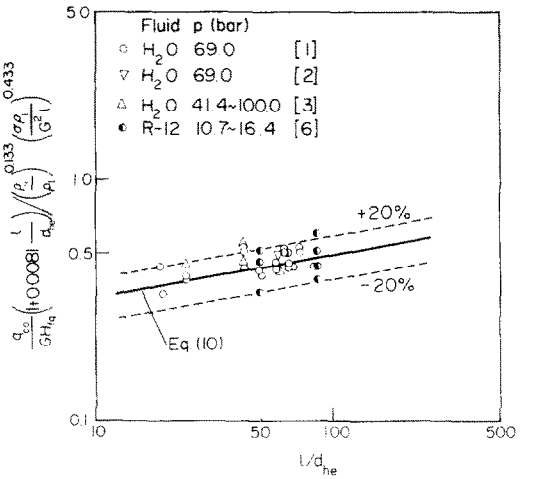

FIG. 6. Nondimensional correlation of q_{c0} in N-regime.

3.6. *HP-regime*

No experiments in HP-regime were made in [1–6], so that the correlation equation of CHF in HP-regime cannot be derived here. Nevertheless, the possibility of HP-regime existing is undeniable, because HP-regime is observed in case of outside heating as shown later in Section 4.3.

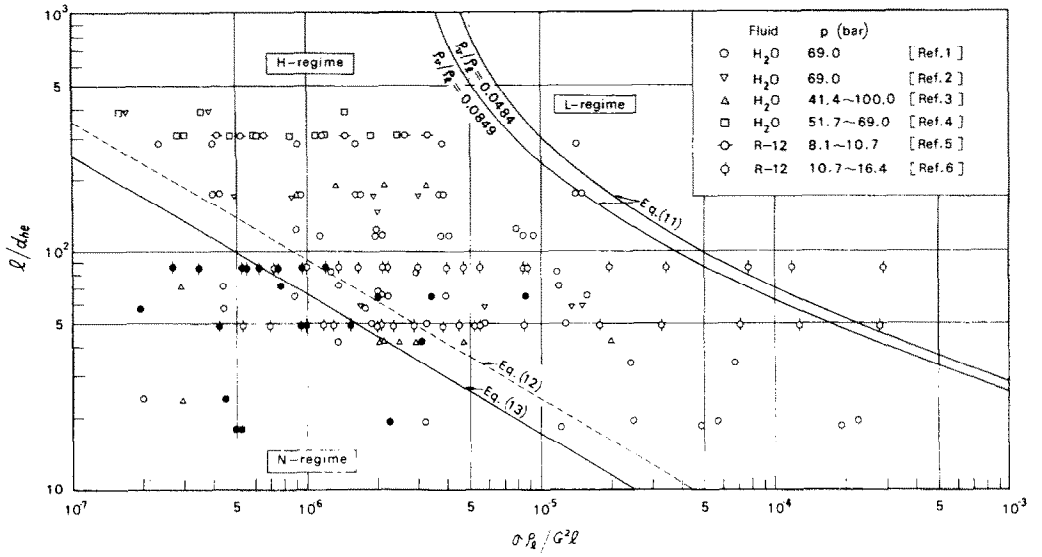

FIG. 7. CHF-regime map for annuli with inside heating.

3.7. *Boundaries of each regime*

By the same means as in case of round tubes, boundaries of each regime are determined. First, the boundary between L- and H-regime is determined by eliminating q_{c0} from equations (8) and (9) as:

$$\frac{l}{d_{he}} = \frac{1}{0.48\left(\frac{\rho_v}{\rho_l}\right)^{0.133}\left(\frac{\sigma\rho_l}{G^2 l}\right)^{0.29} - 0.0081}. \quad (11)$$

Figure 7 shows boundaries predicted by equation (11) for two cases of $\rho_v/\rho_l = 0.0484$ and 0.0849, together with all the data of inside heating which have been so far analyzed in the present paper.

Next, relating to the boundary between H-regime and N-regime, if q_{c0} is eliminated from equations (8) and (10), it yields

$$\frac{l}{d_{he}} = 0.0288\frac{1}{(\sigma\rho_l/G^2 l)^{0.584}} \quad (12)$$

which is represented by the broken line in Fig. 7. However, it is quite apparent that equation (12), corresponding to the point P in Fig. 3, does not indicate the boundary between H- and N-regime. On the other hand, among the data shown in Fig. 7, black symbols represent the data having the non-linear $q_{c0}-\Delta H_i$ relationship (type *B* or *b* in Fig. 2). Since the data of this group are not necessarily sufficient in number, some ambiguities may remain, but if the boundary between H- and N-regime is tentatively determined by the solid, slant line shown in Fig. 7, it yields

$$\frac{l}{d_{he}} = 0.0206\frac{1}{(\sigma\rho_l/G^2 l)^{0.584}}. \quad (13)$$

Equation (13) is the equation which corresponds to equation (A.5) in Appendix for round tubes.

3.8. *Effect of inlet subcooling on CHF*

When liquid is subcooled at the inlet of annuli, critical heat flux q_c in L- and H-regime, where the linear $q_c-\Delta H_i$ relationship holds, can be expressed as follows:

$$q_c = q_{c0}(1+K\Delta H_i/H_{fg}), \quad (14)$$

where K is a dimensionless parameter independent of ΔH_i.

Utilizing the $q_c-\Delta H_i$ relationship obtained from the experimental data of [1–6], K can be determined, and Table 1 lists K in L-regime (designated by K_L) thus obtained. K_L scatters somewhat, but the mean value is $K_L = 1.18$ (which is nearly the same as $K_L = 1.16$ obtained for round tubes in [19]), and therefore the following approximate expression may be permitted:

$$K_L = 1.0. \quad (15)$$

Table 1. Experimental data of K_L

Fluid	p(bar)	l/d_{he}*	$\sigma\rho_l/G^2 l$	K_L
H_2O	69.0	284.2	1.44×10^{-5}	0.74
H_2O	69.0	173.5	1.48×10^{-5}	1.55
H_2O	69.0	172.5	1.42×10^{-5}	1.08
R-12	10.7	85.5	2.91×10^{-4}	1.34
R-12	10.7	85.5	7.66×10^{-5}	1.52
R-12	16.4	85.5	1.19×10^{-4}	0.91
R-12	10.7	49.4	2.80×10^{-4}	1.11
			Average	1.18

*l/d_{he} is given by equation (3).

Next, Fig. 8 shows K in H-regime (designated by K_H) obtained from the experimental data, being correlated in a similar form as that for round tubes [see equation (A.7) in Appendix], and the straight

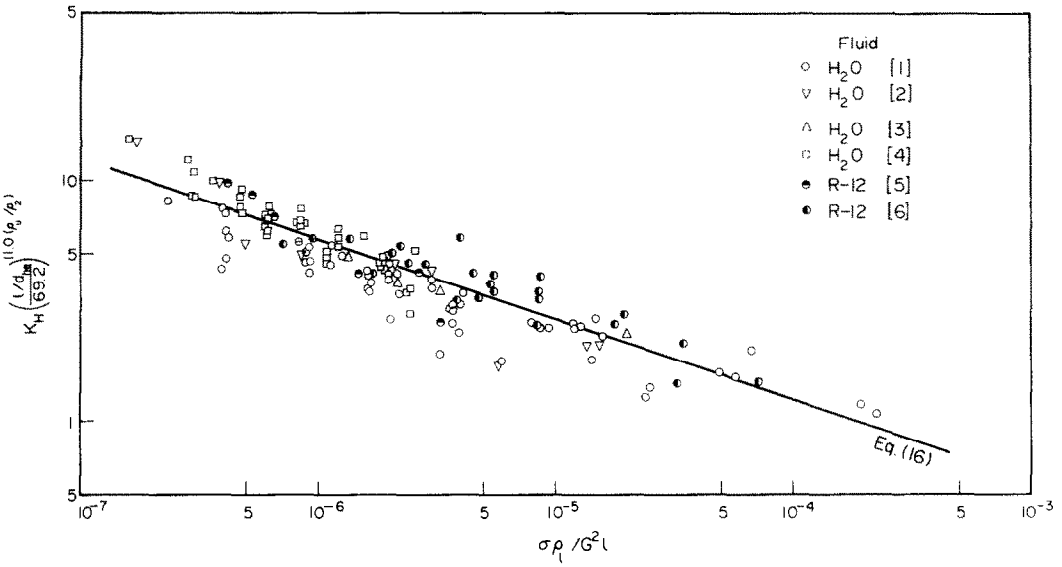

FIG. 8. Correlation of the experimental data of K_H.

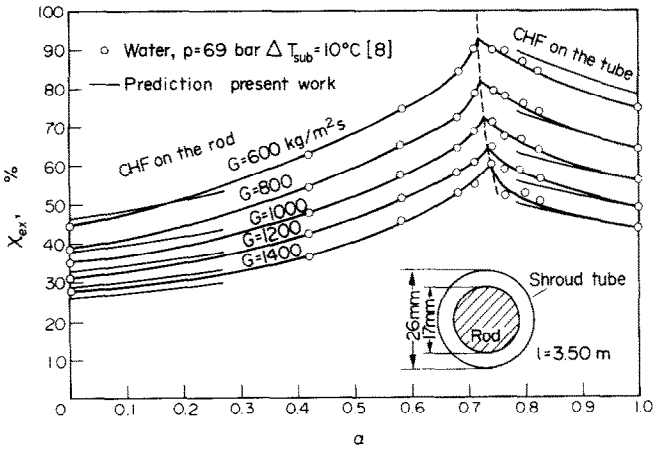

FIG. 9. CHF in bilaterally heated annulus.

line in Fig. 8 is expressed by

$$K_H = 0.057\left(\frac{69.2}{l/d_{he}}\right)^{11.0(\rho_v/\rho_l)}\left(\frac{\sigma\rho_l}{G^2 l}\right)^{-1/3}. \quad (16)$$

In case of round tubes [19], K_H changes its characteristics in the vicinity of $\sigma\rho_l/G^2 l = 3\times10^{-6}$, but no such change is found in case of Fig. 8 for annuli with inside heating.

4. CHF FOR OUTSIDE HEATING

As for CHF in case of outside heating (the rod is unheated and the shroud heated), existing experimental data are few, so that the analysis corresponding to Section 3 cannot be made. Fortunately, however, it seems that only if l/d is replaced by l/d_{he} of equation (4), the correlation equations of CHF for round tubes [equations (A.1)–(A.8) in Appendix] can apply to CHF for annuli with outside heating. Facts illustrative of this rule will be shown below.

4.1. *H-regime*

Figure 9 shows experimental results of exit quality at the state of CHF obtained by Jensen *et al.* [8] for bilaterally heated annuli, where α on the abscissa designates the fraction of total power added to shroud tube, that is

$$\alpha = P_{\text{shroud}}/(P_{\text{rod}} + P_{\text{shroud}}). \quad (17)$$

Therefore, the data for $\alpha = 1$ in Fig. 9 are the data for outside heating, and thereby experimental values of q_c/GH_{fg} for outside heating are readily derived from those data mentioned above through equation (2) [where l/d_{he} is given by equation (4)] to give the result listed in Table 2. On the other hand, according to CHF-regime map given in Fig. 15 of [19], where $C = 0.34$ is now assumed in accordance with the result of [20] for the range of $\sigma\rho_l/G^2 l < 5\times10^{-4}$ (cf. Table 2 in the present text), experiments for $\alpha = 1$ in Fig. 9 are proved to be situated in H-regime.

Table 2. CHF in H-regime for outside heating, corresponding to $\alpha = 1$ in Fig. 9

G (kg/m^2 s)		600	800	1000	1200	1400
	χ_{ex}	0.746	0.640	0.560	0.488	0.437
	$\sigma\rho_l/G^2 l$	1.01×10^{-5}	5.67×10^{-6}	3.63×10^{-6}	2.52×10^{-6}	1.85×10^{-6}
$\frac{q_c}{GH_{fg}}$	Experimental	8.30×10^{-4}	7.17×10^{-4}	6.32×10^{-4}	5.56×10^{-4}	5.01×10^{-4}
	Prediction	8.68×10^{-4}	7.21×10^{-4}	6.25×10^{-4}	5.55×10^{-4}	5.00×10^{-4}

Accordingly, equations (A.2) and (A.7) in Appendix [where l/d is replaced by l/d_{he} of equation (4)] together with equation (14) are used to predict q_c/GH_{fg}, the result of which being listed in the bottom line of Table 2. It is noticed in Table 2 that the agreement between the experimental and the predicted value of q_c/GH_{fg} is very good.

4.2. *N-regime*

Symbols of open circle, black circle and open triangle in Fig. 10 represent experimental data obtained by Ornatskiy *et al.* [11] for outside heating, and it is proved in the similar way as that of the preceding section that the experiments of Fig. 10 belong to N-regime (or quasi N-regime). In addition, as for the data in Fig. 10, it should be noted that most of those data were obtained under conditions of ΔH_i much greater than zero. On the other hand, the symbol x in Fig. 10 represents the prediction of $q_c - \chi_{ex}$ for $\Delta H_i = 0$ by equation (A.3) in Appendix [where l/d is replaced by l/d_{he} of equation (4)] and equation (2). It may be noticed in Fig. 10 that the experimental data for $\Delta H_i < 0$ can be connected to the predicted points for $\Delta H_i = 0$ very smoothly with monotonous curves, and this fact may be regarded to show the applicability of equation (A.3) to predicting CHF in N-regime of outside heating.

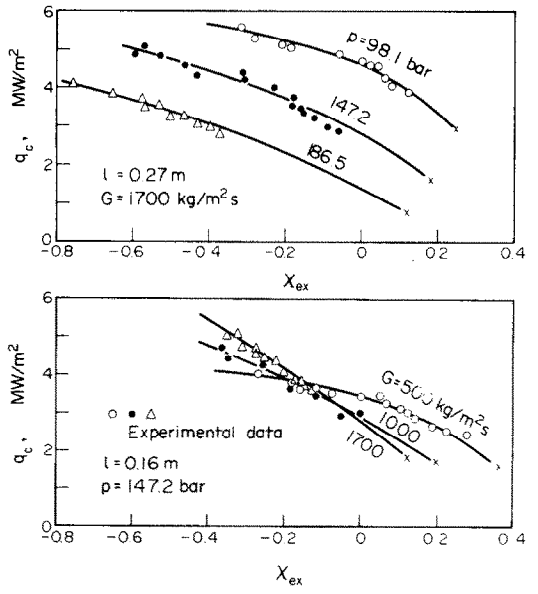

FIG. 10. CHF of water in annuli with outside heating (d_0 = 13 mm and d_i = 10 mm). Comparison between data of [11] and the prediction (x) of equations (A.3) and (2).

4.3. *HP-regime*

Data of water at 216 bars (very near the critical point of water) presented by Ornatskiy *et al.* [9] show the linear $q_c - \Delta H_i$ relationship, and q_{c0} can be obtained by extrapolating q_c as $\Delta H_i \to 0$ to give the data shown in Fig. 11. On the other hand, in the similar way as before, it is proved that the experiments of Fig. 11 are situated thoroughly in HP-regime, and this does not contradict the linear $q_c - \Delta H_i$ relationship mentioned before. Therefore, the prediction of q_{c0}/GH_{fg} by equation (A.4) should be compared with the experimental data in Fig. 11, and it shows a fairly good agreement. For caution's sake, in Fig. 11 are also shown the prediction by equations (A.2) and (A.3) for H- and N-regime respectively, showing noticeable disagreements with the experimental data.

Supplementary note. Ornatskiy *et al.* [9] observed that CHF was not affected by the width of annular channel in their experimental range, while the prediction of equation (A.4) results in a dispersion such as shown by a solid and a broken curve in Fig. 11. In addition, K_{HP} determined from experimental data of Ornatskiy *et al.* has considerably different values from the prediction of equation (A.8). On these discrepancies, further study will be necessary for clarifying causes.

5. CHF FOR BILATERAL HEATING

5.1. *Approximate method for prediction of CHF in L- and H-regime*

When the shroud of an annulus is heated in the ratio of α defined in equation (17), the annular channel may be divided by an imaginary cylindrical surface of diameter d_m as shown in Fig. 12 so as to proportion the cross-sectional area of each sub-channel to the heat load of the wall adjoining the sub-channel, that is

$$(d_0^2 - d_m^2)/(d_m^2 - d_i^2) = P_{\text{shroud}}/P_{\text{rod}}. \tag{18}$$

Then, eliminating $P_{\text{shroud}}/P_{\text{rod}}$ from equations (17) and (18), it yields

$$(d_m/d_i)^2 = \alpha + (1-\alpha)(d_0/d_i)^2. \tag{19}$$

Now, it is boldly assumed that the mass velocity and the axial flow rate of energy are uniform all over the cross-section of annulus, when the transport of mass and energy across the imaginary cylindrical surface can vanish making no alterations to the flow. Then, the inner sub-channel can be regarded as an annulus with inside heating, for which the heated equivalent diameter d_{he} is given from the definition of

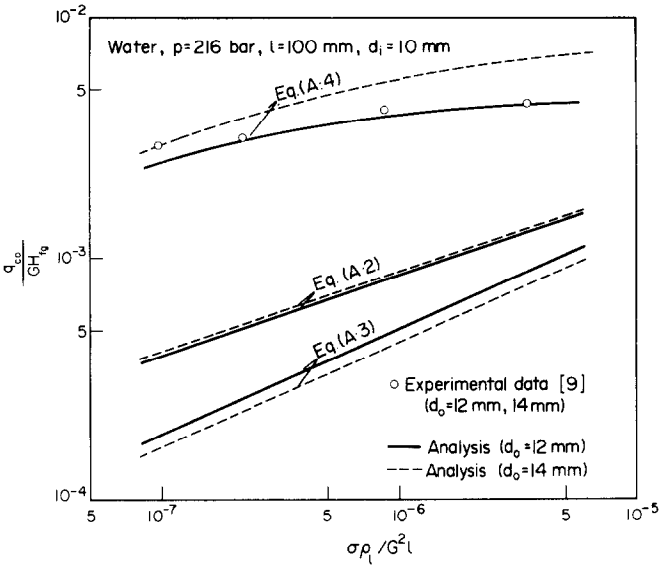

FIG. 11. CHF of water in annuli with outside heating.

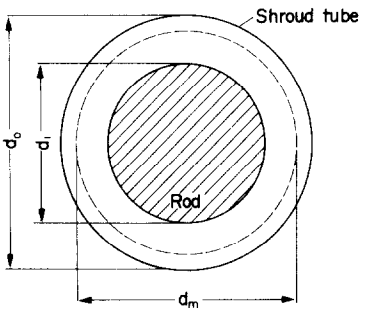

FIG. 12. Division of an annular channel.

equation (1) as $d_{he} = (d_m^2 - d_i^2)/d_i$. Similarly, the outer sub-channel can be regarded as an annulus with outside heating, for which the heated equivalent diameter is given from equation (1) as $d_{he} = (d_0^2 - d_m^2)/d_0$. Consequently, eliminating d_m from these two relations and equation (19), it yields:

for inner sub-channel:

$$\frac{l}{d_{he}} = \frac{1}{1-\alpha} \cdot \frac{l}{d_i} \cdot \frac{1}{(d_0/d_i)^2 - 1}; \tag{20}$$

for outer sub-channel:

$$\frac{l}{d_{he}} = \frac{1}{\alpha} \cdot \frac{l}{d_i} \cdot \frac{d_o/d_i}{(d_0/d_i)^2 - 1}. \tag{21}$$

Equation (20) reduces to equation (3) when $\alpha = 0$, and equation (21) reduces to equation (4) when $\alpha = 1$.

Then, when α is near zero, CHF on the rod may be predicted approximately by applying l/d_{he} of equation (20) to correlation equations (8)–(16). For example, in case of experiments of Fig. 9, they are proved to be situated in H-regime for $\alpha \doteqdot 0$, and therefore χ_{ex} is predicted by equations (2), (8), (14), (16) and (20), yielding thin curves in the range of $\alpha = 0$–0.27 in Fig. 9. Similarly, when α is near unity, CHF on the shroud may be predicted approximately by applying l/d_{he} of equation (21) to correlation equations (A.1)–(A.8) in Appendix. For example, in case of the experiments of Fig. 9, they are proved to be situated in H-regime for $\alpha \doteqdot 1$, and therefore χ_{ex} is predicted by equations (2), (14), (20), (A.2) and (A.7), yielding thin curves in the range of $\alpha = 0.8 - 1.0$ in Fig. 9. Besides, it may be of use to note that similar results as above are also obtained for the experiments of Jensen *et al.* [8] with inlet subcooling temperature $\Delta T_{sub} = 100°C$. In sum, the above-mentioned approximate method for predicting CHF for bilateral heating in the vicinity of $\alpha = 0$ and 1 may be regarded as useful considering its extreme simplicity.

As for the experimental data of Becker *et al.* [7], inlet subcooling enthalpy ΔH_i (or mass velocity G) is not given, so that quantitative comparisons cannot be made. However, their data seem to have the similar trend as that shown in Fig. 9, and moreover, their experimental range extends over L- and H-regime. Therefore, it might be presumed that the above-mentioned method of predicting CHF is effective in L-regime too.

5.2. *Circumstances in HP-regime*

Ornatskiy *et al.* [9], who presented the data shown in Fig. 11, carried out experiments for $\alpha = 0.6$–0.7 at the pressure of 172–216 bars, giving the conclusion that the heating rod had no effect on the CHF on shroud. Tolubinskiy *et al.* [10] also made experiments for $\alpha = 0$–0.5 at the pressure of 150 and 200 bars, giving the conclusion that the heating of shroud had no effect on the CHF on rod. As for the data given by Tolubinskiy *et al.*, those at 150 bars belongs to H-regime, but it can be presumed that the data at 200 bars is situated in HP-regime, because when they are examined by the same method as that

used in Fig. 10, it is found that they belong to neither H-regime nor N-regime. Therefore, according to the above two papers at least, it seems likely that there is no interference between rod and shroud for CHF in HP-regime.

6. CONCLUSIONS

(i) For annuli with inside heating, the existing experimental data of CHF (water and Freon-12) are analyzed to give equations (8)–(10) for the correlation of CHF at zero inlet subcooling, Fig. 7 for the CHF-regime map, and equations (15) and (16) for the effect of inlet subcooling on CHF. Geometrical factors concerned are the heated equivalent diameter of equation (3) and the length of annuli. No correlation in HP-regime is derived for the lack of experimental data.

(ii) For outside heating, it is shown that only if l/d is replaced by l/d_{he} of equation (4), the correlation for round tubes [equations (A.1)–(A.8) in Appendix] applies to the prediction of CHF without any other modifications.

(iii) For bilateral heating, an approximate method is presented for predicting CHF in L- and H-regime in the vicinity of $\alpha = 0$ and $\alpha = 1$. As for CHF in HP-regime, it is suggested that the interference between the rod and shroud may disappear.

Acknowledgements The author wishes to pay his respects to all the authors reporting the experimental data used in this study, and the financial support provided by the Ministry of Education is gratefully acknowledged.

REFERENCES

1. P. G. Barnett, A correlation of burnout data for uniformly heated annuli and its use for predicting burnout in uniformly heated rod bundles, AEEW-R463 (1966).
2. P. G. Barnett, A comparison of the accuracy of some correlations for annuli and rod bundles, AEEW-R558 (1968).
3. E. Janssen and J. A. Kervinen, Burnout conditions for single rod in annular geometry, GEAP-3899 (1963).
4. R. B. Little, Dryout tests on an internally heated annulus with variation of axial heat flux distribution, AEEW-R578 (1970).
5. G. F. Stevens, R. W. Wood and J. Pryzbyski, An investigation into the effect of a cosine axial heat flux distribution on burnout in a 12 ft long annulus using Freon-12, AEEW-R609 (1968).
6. S. Y. Ahmad and D. C. Groeneveld, Fluid modelling of critical heat flux in uniformly heated annuli, *International Symposium on Two-Phase Systems*, Haifa (1971), Paper 1-8; or AECL-4070 (1972).
7. K. M. Becker and G. Hernborg, Measurements of burnout conditions for flow of boiling water in a vertical annulus, *J. Heat Transfer* **86**, 393 (1964).
8. A. Jensen and G. Mannov, Measurements of burnout film thickness and pressure drop in a concentric annulus 3500 × 26 × 17 mm with heated rod and tube, *European Two-Phase Flow Group Meeting*, Harwell (1974).
9. A. P. Ornatskiy, L. F. Glushchenko and A. M. Kichigin, Burnout in annular channels with two-sided heating, *Heat Transfer—Soviet Res.* **1**(6), 12 (1969).
10. V. I. Tolubinsky, A. K. Litoshenko, V. L. Shevtsov, Ye. D. Domashev and G. Ye. Struchenko, Heat transfer crisis at the inward surface of annuli heated from both sides, *Heat Transfer—Soviet Res.* **5**(3), 93 (1973).
11. A. P. Ornatskiy, V. A. Chernobay, A. P. Vasil'yev and S. V. Perkov, Critical heat fluxes in annuli with swirl, *Heat Transfer—Soviet Res.* **7**(2), 6 (1975).
12. L. S. Tong, H. B. Currin and F. C. Engel, DNB (burnout) studies in an open lattice core, WCAP-3736 (1964).
13. S. Bertoletti, G. P. Gaspari, C. Lombardi, G. Peterlongo, M. Silvestri and F. A. Tacconi, Heat transfer crisis with steam–water mixtures, *Energie Nucleare* **12**, 121 (1965).
14. K. M. Becker, A correlation for burnout predictions in vertical rod bundles, S-349 (1966).
15. G. F. Hewitt, H. A. Kearsy and J. G. Collier, Correlation of critical heat flux for the vertical flow of water in uniformly heated channels, AERE-5590 (1970).
16. S. Y. Ahmad and D. C. Groeneveld, Fluid modelling of critical heat flux in uniformly heated annuli, *Progress in Heat and Mass Transfer*, Vol. 6 p. 45. Pergamon Press, Oxford (1972).
17. V. I. Tolubinskiy, Ye. D. Demashev, A. K. Litoshenko and A. S. Matorin, Boiling crisis in concentric and eccentric annuli, *Heat Transfer—Soviet Res.* **9**(1), 132 (1977).
18. A. P. Ornatskiy, V. A. Chernobay, S. V. Perkov and A. F. Vasil'yev, Correlation of data on heat transfer crisis in annuli on basis of flow parameters at the inlet, *Heat Transfer—Soviet Res.* **8**(3), 37 (1976).
19. Y. Katto, A generalized correlation of critical heat flux for the forced convection boiling in vertical uniformly heated round tubes, *Int. J. Heat Mass Transfer* **21**, 1527 (1978).
20. Y. Katto, A generalized correlation of critical heat flux for the forced convection boiling in vertical uniformly heated round tubes—a supplementary report. *Int. J. Heat Mass Transfer*, to be published.

APPENDIX

Correlation equations of CHF derived by the author [19, 20] for round tubes in case of $\Delta H_i = 0$ are as follows:

L-regime:

$$\frac{q_{c0}}{GH_{fg}} = C\left(\frac{\sigma\rho_l}{G^2 l}\right)^{0.043}\frac{1}{l/d}, \tag{A.1}$$

where $C = 0.34$ for $\sigma\rho_l/G^2 l < 5\times10^{-4}$ and $C = 0.25$ for $5\times10^{-4} < \sigma\rho_l/G^2 l$.

H-regime:

$$\frac{q_{c0}}{GH_{fg}} = 0.10\left(\frac{\rho_v}{\rho_l}\right)^{0.133}\left(\frac{\sigma\rho_l}{G^2 l}\right)^{1/3}\frac{1}{1+0.0031 l/d}. \tag{A.2}$$

H- and N-regime:

$$\frac{q_{c0}}{GH_{fg}} = 0.098\left(\frac{\rho_v}{\rho_l}\right)^{0.133}\left(\frac{\sigma\rho_l}{G^2 l}\right)^{0.433}\frac{(l/d)^{0.27}}{1+0.0031 l/d}. \tag{A.3}$$

HP-regime:

$$\frac{q_{c0}}{GH_{fg}} = 8.20\left(\frac{\rho_v}{\rho_l}\right)^{0.65}\left(\frac{\sigma\rho_l}{G^2 l}\right)^{0.453}\frac{1}{1+107\left(\frac{\sigma\rho_l}{G^2 l}\right)^{0.54}\frac{l}{d}}. \tag{A.4}$$

With respect to equation (A.3), the boundary between H- and N-regime is given by

$$\frac{d}{l} = 0.77\frac{1}{(\sigma\rho_l/G^2 l)^{0.37}}. \tag{A.5}$$

Next, K in equation (14) of the text in case of $\Delta H_i > 0$ is given as follows:

L-regime: $K_L = 1$ (A.6)

H-regime:

$$\left.\begin{array}{l}\text{for } \sigma\rho_l/G^2l < 3\times10^{-6},\\ \quad K_H = 1.8\left(\dfrac{130}{l/d}\right)^{5.0(\rho_v/\rho_l)}\\ \text{for } 3\times10^{-6} < \sigma\rho_l/G^2l,\\ \quad K_H = 0.075\left(\dfrac{130}{l/d}\right)^{5.0(\rho_v/\rho_l)}\left(\dfrac{\sigma\rho_l}{G^2l}\right)^{-1/4}\end{array}\right\} \quad \text{(A.7)}$$

HP-regime:

$$\left.\begin{array}{l}\text{for } \sigma\rho_l/G^2l < 4\times10^{-8},\\ \quad K_{HP} = 0.664(\rho_v/\rho_l)^{-0.6}\\ \text{for } 4\times10^{-8} < \sigma\rho_l/G^2l,\\ \quad K_{HP} = 3.08(\sigma\rho_v/G^2l)^{0.09}(\rho_v/\rho_l)^{-0.6}.\end{array}\right\} \quad \text{(A.8)}$$

FORMULATIONS GENERALES POUR LE FLUX THERMIQUE CRITIQUE EN EBULLITION AVEC CONVECTION FORCEE DANS DES ESPACES ANNULAIRES VERTICAUX ET UNIFORMEMENT CHAUFFES

Résumé—Suivant la procédure analytique appliquée par l'auteur au cas du flux thermique critique (CHF) dans les tubes circulaires, on analyse les données expérimentales du CHF dans les espaces annulaires avec chauffage au centre, pour obtenir une formule générale du CHF dans ce type de chauffage. Comme pour l'espace annulaire avec chauffage externe, on montre que le CHF peut être convenablement représenté en utilisant la formation générale de l'auteur concernant le CHF pour les tubes circulaires. Les estimations du CHF dans les deux cas peuvent être établies en employant le diamètre caractéristique de l'anneau. On discute aussi le cas des anneaux chauffés sur les deux frontières et on présente une méthode approchée pour le calcul du CHF dans les régimes bas ou forts, tandis que l'interférence entre les deux parois disparait dans le régime HP.

ALLGEMEINGÜLTIGE BEZIEHUNGEN FÜR DIE KRITISCHE WÄRMESTROMDICHTE BEIM SIEDEN MIT ERZWUNGENER KONVEKTION IN SENKRECHTEN, GLEICHMÄSSIG BEHEIZTEN RINGRÄUMEN

Zusammenfassung—Es wurden vorliegende experimentelle Daten für die kritische Wärmestromdichte (KWD) in Ringräumen mit beheizter Innenseite analysiert, um eine allgemeingültige Beziehung für die KWD bei dieser Art der Beheizung zu erhalten. Dabei wurde ein analytisches Verfahren nach dem gleichen Prinzip angewandt, wie es vom Autor für die Untersuchung der KWD für runde Rohre verwendet wurde. Es wird gezeigt, daß die KWD für Ringräume mit beheizter Außenseite ohne weiteres mit Hilfe der allgemeinen Beziehung des Autors für die KWD runder Rohre berechnet werden kann. Die Berechnung der KWD in den beiden oben erwähnten Fällen kann durchgeführt werden, wenn man den beheizten äquivalenten Durchmesser allein als repräsentativen Durchmesser der Ringräume verwendet. Schließlich wird auch der Fall der beidseitig beheizten Ringräume diskutiert und eine Näherungsmethode für die Berechnung der KWD im L- und H-Bereich angegeben, während beim HP-Bereich zu bedenken ist, daß die Wechselwirkung zwischen den beiden Wänden bezüglich der KWD cerschwindet.

ОБОБЩЕННЫЕ ЗАВИСИМОСТИ ДЛЯ КРИТИЧЕСКОГО ТЕПЛОВОГО ПОТОКА ПРИ КИПЕНИИ С ВЫНУЖДЕННОЙ КОНВЕКЦИЕЙ В ВЕРТИКАЛЬНЫХ РАВНОМЕРНО НАГРЕВАЕМЫХ КОЛЬЦЕВЫХ КАНАЛАХ

Аннотация — С помощью того же аналитического метода, который использовался при исследовании критического теплового потока (КТП) для круглых труб, проведен анализ имеющихся экспериментальных данных по КТП в кольцевых каналах с внутренним нагревом и дано обобщенное соотношение для КТП, которое соответствует этому типу нагрева. Для кольцевых каналов с внешним нагревом показано, что КТП можно легко рассчитать с помощью предложенного автором обобщенного соотношения для круглых труб. Для расчёта КТП в обоих случаях достаточно заменить диаметр кольцевых каналов эквивалентным диаметром нагрева. Наконец, рассмотрен двухсторонний нагрев кольцевых каналов и приведен приближенный метод расчёта КТП для режимов L и H в предположении, что взаимное влияние стенок несущественно для КТП в режиме HP.